Journal of Medicinal Chemistry

Brief Article

pubs.acs.org/jmc

The Extracellular Entrance Provides Selectivity to Serotonin 5-HT$_7$ Receptor Antagonists with Antidepressant-like Behavior in Vivo

Rocío A. Medina,[†,⊥] Henar Vázquez-Villa,[†,⊥] José C. Gómez-Tamayo,[‡] Bellinda Benhamú,[†] Mar Martín-Fontecha,[†] Tania de la Fuente,[†,∥] Gianluigi Caltabiano,[‡] Peter B. Hedlund,[§] Leonardo Pardo,*[,‡] and María L. López-Rodríguez*[,†]

[†]Departamento de Química Orgánica I, Facultad de Ciencias Químicas, Universidad Complutense de Madrid, E-28040 Madrid, Spain

[‡]Laboratori de Medicina Computacional, Unitat de Bioestadística, Facultat de Medicina, Universitat Autònoma de Barcelona, E-08193 Bellaterra, Barcelona, Spain

[§]Department of Cellular and Molecular Neuroscience, The Scripps Research Institute, La Jolla, California 92037, United States

Supporting Information

ABSTRACT: The finding that ergotamine binds serotonin receptors in a less conserved extended binding pocket close to the extracellular entrance, in addition to the orthosteric site, allowed us to obtain 5-HT$_7$R antagonist **6** endowed with high affinity (K_i = 0.7 nM) and significant 5-HT$_{1A}$R selectivity (ratio >1428). Compound **6** exhibits in vivo antidepressant-like effect (1 mg/kg, ip) mediated by the 5-HT$_7$R, which reveals its interest as a putative research tool or pharmaceutical in depression disorders.

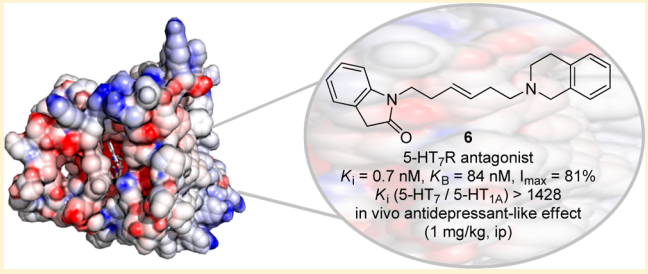

INTRODUCTION

The serotonin (5-hydroxytryptamine, 5-HT) 5-HT$_7$ receptor (5-HT$_7$R), first cloned in 1993,[1,2] is distributed in discrete areas of the brain and in the periphery.[3] Within the central nervous system (CNS), particularly high levels have been detected in the thalamus, hippocampus, and hypothalamus (especially within the suprachiasmatic nucleus). To date, the functional role of the 5-HT$_7$R in various pathophysiological processes has been described.[3−6] For instance, activation of the 5-HT$_7$R is involved in nociceptive processing, and it has been proposed that agonists of the receptor could be used as adjuvant drugs in pain treatment.[7,8] Results from animal models of learning and memory have suggested that the 5-HT$_7$R represents a potential therapeutic target for the treatment of memory dysfunction in cognitive disorders (schizophrenia, Alzheimer's disease, and age-related decline).[9,10] On the other hand, pharmacological blockade or genetic inactivation of the 5-HT$_7$R leads to an antidepressant-like behavioral profile in vivo.[11,12] It has also been suggested that the clinically established antidepressant effect of atypical antipsychotic drugs amisulpride and lurasidone is due to their blockade of the 5-HT$_7$R.[13,14]

Major depression is a common psychiatric disorder associated with high symptomatic and functional burdens. Pharmacological treatment is often effective, but there remain substantial unmet needs in the form of nonresponders, delayed onset of clinical effect, and side effects. In recent decades, an increasing demand has emerged for the discovery of new types of antidepressants. The therapy of this psychiatric disease is dominated by selective serotonin reuptake inhibitor (SSRI) antidepressants. However, the main drawback of this class of drugs is to produce a therapeutic effect only after several weeks of treatment. Importantly, a recent study showed that the pharmacological blockade of the 5-HT$_7$R produces a faster antidepressant-like response than the 5-HT uptake inhibitor fluoxetine, commonly used as an antidepressant agent.[15] Therefore, 5-HT$_7$R antagonists could represent a possible alternative to SSRIs as antidepressant drugs with a faster onset of action. All together, these studies have positioned the 5-HT$_7$R as a promising drug target in the search for new antidepressant agents. Indeed, several antagonists of the receptor induce an antidepressant-like behavior in preclinical models of depression.[16−18] Interestingly, 5-HT$_7$R antagonist SB-269970 (3-({(2*R*)-2-[2-(4-methylpiperidin-1-yl)ethyl]-pyrrolidin-1-yl}sulfonyl)phenol) also potentiates the effect of clinically used antidepressants such as citalopram, imipramine, desipramine, and moclobemide,[19,20] and JNJ-18038683 (3-(4-chlorophenyl)-1,4,5,6,7,8-hexahydro-1-(phenylmethyl)-pyrazolo[3,4-*d*]azepine 2-hydroxy-1,2,3-propanetricarboxylate) has been evaluated in a clinical trial (phase 2) for the treatment of major depressive disorder.[21] This boosts the efforts toward the development of new 5-HT$_7$R antagonists that are still needed to validate their suitability as therapeutic agents.

In this context, our research group has previously identified a structurally new family of 5-HT$_7$R ligands represented by **1** and **2** (Chart 1).[22,23] However, the demonstrated close similarities between the binding sites of 5-HT$_7$ and 5-HT$_{1A}$ receptors have resulted in difficulties in developing selective 5-HT$_7$R

Received: June 10, 2014
Published: July 29, 2014

ACS Publications © 2014 American Chemical Society

dx.doi.org/10.1021/jm500880c | *J. Med. Chem.* 2014, 57, 6879−6884

Chart 1

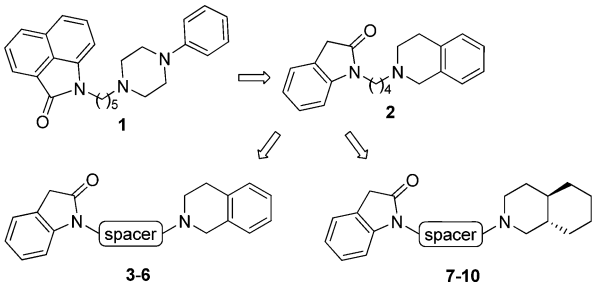

agents.[18,24−26] Thus, in this work we have focused our efforts in obtaining ligands endowed with 5-HT$_7$/5-HT$_{1A}$ receptor selectivity. We took advantage of the increasing number of available crystal structures of the G protein-coupled receptor (GPCR) family,[27] to which 5-HT$_{1A}$ and 5-HT$_7$ receptors belong. All these structures share the common architecture of seven transmembrane domains (TMs),[28] forming a water-filled binding-site crevice. Moreover, the recent crystal structures of ergotamine bound to 5-HT$_{1B}$ and 5-HT$_{2B}$ receptors have revealed a large ligand binding cavity defined by the regular orthosteric pocket within TMs 3, 5, 6, and 7 and extracellular loop (ECL) 2, embedded deep in the 7TM core, and an extended binding pocket close to the extracellular entrance.[29,30] Because this extracellular entrance is less conserved than the orthosteric binding site,[31] this finding opens the opportunity to obtain ligands with significant subtype selectivity. Compound **2**, previously reported in our laboratory,[23] showed high binding affinity for the 5-HT$_7$R (K_i = 7 nM) and moderate selectivity (5-HT$_7$/5-HT$_{1A}$ ratio = 31). This compound was predicted to bind in the conserved orthosteric pocket within TMs 3, 5, and 6.[23] Because the 7TM bundle limits the length of this orthosteric pocket between TMs 3 (D3.32) and 5 (S5.42), we designed compounds **3**−**10** (Chart 1) that contain increasing number of methylene units in the spacer with the aim of improving receptor selectivity. In particular, analogue **6** has been characterized as a potent and selective 5-HT$_7$R antagonist that exhibits in vivo antidepressant activity in the tail suspension and the forced swim tests.

RESULTS AND DISCUSSION

In the design of compounds **3**−**10** (Chart 1, Table 1), the main idea was that derivatives with a small number of methylene units (short spacers) would fit the protonated amine and the indolone moieties of the ligand within the orthosteric site, showing moderate selectivity due to a conserved pocket (Figure 1A, top panel). In contrast, compounds with a large number of methylene units (long spacers) would reverse the binding mode so that the protonated amine binds D3.32 in the orthosteric site and the indolone moiety would expand toward the extracellular entrance where sequence divergences between 5-HT$_7$ and 5-HT$_{1A}$ receptors are observed (Figure 1A, bottom panel).

Target compounds **3**−**10** were synthesized starting from commercially available 1,3-dihydro-2*H*-indol-2-one. Alkylation with the appropriate dibromide derivative in the presence of K_2CO_3 afforded bromoalkanes **11**−**15**. These intermediates were subsequently treated with 1,2,3,4-tetrahydroisoquinoline or (±)-*trans*-decahydroisoquinoline using triethylamine and acetonitrile as solvent to obtain final compounds **3**−**6** or **7**−**10**, respectively (Scheme 1).

Table 1. 5-HT$_7$ and 5-HT$_{1A}$ Receptors Affinities of New Synthesized Compounds 3−10

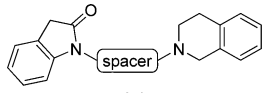

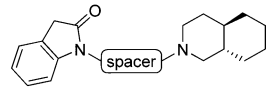

Compd	Spacer	K_i ± SEM (nM)[a]	
		5-HT$_7$[b]	5-HT$_{1A}$[c]
2	$(CH_2)_4$	7 ± 2[d]	219 ± 11[d]
3	$(CH_2)_5$	28 ± 6	523 ± 7
4	$(CH_2)_6$	24 ± 3	576 ± 8
5	$(CH_2)_7$	36 ± 3	> 1000
6	$(CH_2)_2$-CH=CH-$(CH_2)_2$	0.7 ± 0.3	> 1000
7	$(CH_2)_4$	29 ± 5	470 ± 5
8	$(CH_2)_5$	41 ± 8	491 ± 3
9	$(CH_2)_7$	62 ± 7	> 1000
10	$(CH_2)_2$-CH=CH-$(CH_2)_2$	2.7 ± 0.7	> 1000

[a]Values are the mean of two to four experiments performed in triplicate. [b]5-CT was used as a reference compound (K_i = 1.8 ± 0.6 nM). [c]8-OH-DPAT was used as a reference compound (K_i = 1.02 ± 0.08 nM). [d]Value from ref 23.

Affinity of compounds **3**−**10** for studied serotonin receptors was evaluated by radioligand competitive binding assays using membranes of CHO-K1 or HEK-293 cells transfected with human 5-HT$_7$ or 5-HT$_{1A}$ receptors and [^{3}H]LSD or [^{3}H]-8-OH-DPAT, respectively. The affinity constants K_i calculated from the inhibitory concentration 50 (IC_{50}) are shown in Table 1. All synthesized compounds bind the 5-HT$_7$R and tetrahydroisoquinoline derivatives (**2**−**6**) display higher affinity than the corresponding decahydroisoquinoline analogues (**7**−**10**). Notably, an increase in the number of methylene units in the spacer in compounds **2**−**5** and **7**−**9** leads to an improvement of the selectivity against the 5-HT$_{1A}$R. Moreover, compounds **6** and **10** containing a 3-hexenylene spacer exhibit higher 5-HT$_7$R affinity (K_i = 0.7 and 2.7 nM, respectively) than a hexylene analogue **4** (K_i = 24 nM). Clearly, **6** and **10** displayed the best profiles of both 5-HT$_7$R affinity and 5-HT$_7$/5-HT$_{1A}$ selectivity (ratios >1428 and 370, respectively). In these ligands, the double bond of the spacer mimics the planar conformation of the carboxamide group of ergotamine (Figure 1B). Thus, these experimental data suggest that 3-hexenylene spacer, as well as seven-methylene units, trigger the reverse binding mode toward the extracellular entrance. Moreover, the enhanced binding affinity of **6** (K_i = 0.7 nM), relative to **2** (K_i = 7 nM), shows that the indolone moiety optimally binds this cavity. In an attempt to characterize the amino acid residues of the extracellular entrance involved in the recognition of the indolone moiety, we performed molecular dynamics (MD) simulations of the complex between compound **6** and a 5-HT$_{1B}$R-based homology model of the 5-HT$_7$R (see Experimental Section and Figure 1C). Importantly, the interaction between the protonated amine and D3.32 remains stable through the simulation time, while the indolone moiety accomplishes key interactions with R6.58 and R7.36 at the extracellular entrance. The fact that the 5-HT$_{1A}$R replaces these charged amino acids by Leu and Ala, respectively, explains the observed selectivity. In detail, E7.35 and Q23$5^{i+4}$ in ECL 2 maintain R6.58 toward the extracellular entrance to interact

dx.doi.org/10.1021/jm500880c | J. Med. Chem. 2014, 57, 6879−6884

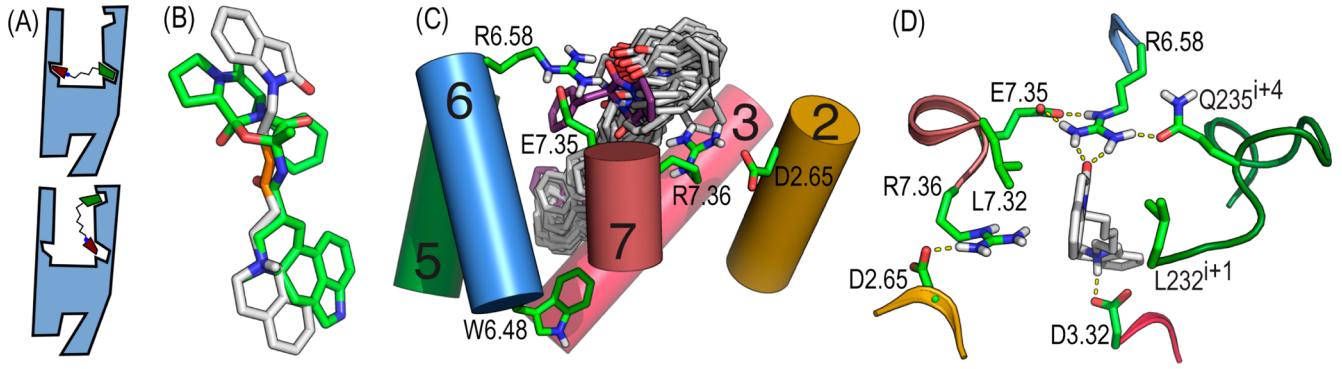

Figure 1. MD simulations of the 5-HT$_7$R in complex with compound **6**. (A) Potential modes of binding of ligands **2**–**10**. Derivatives with short spacers would bind within the orthosteric site, between TMs 2 and 5[22,23] (top panel), whereas derivatives with large spacers would bind both at the orthosteric site and at the extracellular entrance (bottom panel). (B) Superimposition of ergotamine (in green) and compound **6** (in white). The position of the double bond of **6**, to mimic the planar conformation of the carboxamide group of ergotamine, is shown in orange. (C) The structures of **6** (in white) computed during the simulation (50 structures collected every 2 ns). Superimposition of ergotamine (in purple), as found in the crystal structure of the 5-HT$_{1B}$R, shows that both compounds bind the receptor in a similar manner. (D) Detailed view of the interaction of **6** with D3.32, L232^{i+1} (at position i + 1 relative to the conserved C231^{i} engaged in a disulfide bond with C3.25 in TM 3), R6.58, L7.32, and R7.36.

Scheme 1. Synthesis of Target Compounds 3–10[a]

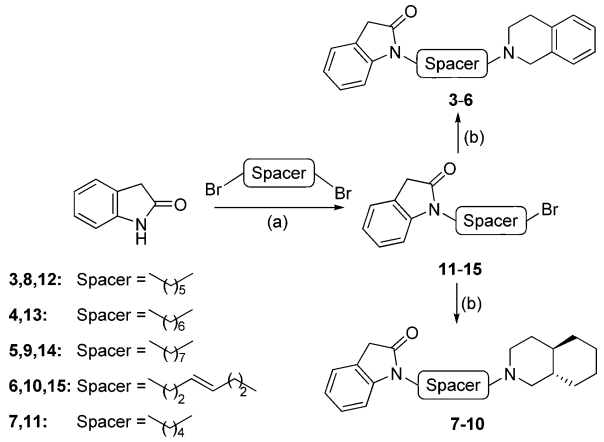

[a]Reagents and conditions: (a) K_2CO_3, CH_3CN, reflux, 20 h, 30–77%; (b) 1,2,3,4-tetrahydroisoquinoline or (±)-*trans*-decahydroisoquinoline, Et_3N, CH_3CN, 60 °C, 24 h, 67–81%.

with the carbonyl group of the indolone moiety, while the aromatic ring is located between L232^{i+1} and L7.32 and forms a cation–π interaction with R7.36 (Figure 1D).

Subsequently, functional characterization of selective ligands **6** and **10** was assessed by evaluating their effect on adenylate cyclase (AC) activity in CHO cells expressing the human 5-HT$_7$R. Treatment with the ligand caused a dose-dependent increase in cAMP levels, although a low effect in maximum activation, was observed in both cases (E_{max} = 21% and 36%, respectively, Table 2). After pretreatment with serotonin, the new compounds induced a dose-dependent decrease of cAMP concentration, and maximum inhibitory effects (I_{max}) of 81 and 66% were attained, respectively (Table 2). The concentration values that produce half of that effect, IC_{50}, and the calculated dissociation constants, K_B, are shown in Table 2. These data indicate that ligands **6** and **10** exhibit in vitro antagonist character at the human 5-HT$_7$R in the AC assay.

Table 2. Functional Activity of High-Affinity 5-HT$_7$R Ligands

ligand	EC_{50} (μM)	E_{max} (%)	IC_{50} (μM)	K_B (nM)	I_{max} (%)
6	0.23	21	2.2	84	81
10	0.06	36	2.3	88	66
5-HT	0.017				
Mesulergine			0.29	11	

Altogether, the newly identified 5-HT$_7$R antagonist **6** displays an optimized profile in terms of affinity (K_i = 0.7 nM), selectivity (5-HT$_7$/5-HT$_{1A}$ ratio >1428), and functional activity (K_B = 84 nM, I_{max} = 81%).

To further characterize compound **6**, we assessed its antagonist character in vivo by determining its effect on hypothermia induced by reference agonist 8-OH-DPAT in mice. Core body temperature was measured using a rectal probe thermometer. A basal value was measured, immediately before any intraperitoneal (ip) injection, and changes in body temperature were determined as peak effect (maximum change during the first 30 min) and overall effect (area under the curve for the total registration period of 2 h). As shown in Figure 2, 8-OH-DPAT (0.3 mg/kg, ip) induced hypothermia, as expected, in contrast to tested compound **6** (0.3 and 1 mg/kg) that had no effect on body temperature by itself. Importantly, the hypothermic effect of 8-OH-DPAT could be counteracted by compound **6** when administered at the dose of 1 mg/kg 30 min before 8-OH-DPAT (Figure 2). It has been previously found that at the dose used (0.3 mg/kg), 8-OH-DPAT acts mainly as a 5-HT$_7$R agonist.[32] Therefore, the ability of **6** to inhibit the hypothermic effect of 8-OH-DPAT indicates that the high-affinity ligand identified herein acts as a 5-HT$_7$R antagonist in vivo.

The pharmacological action of the new 5-HT$_7$R antagonist **6** was evaluated in the tail suspension and forced swim tests, two mouse models in which an antidepressant behavior is attributed to a decrease in the immobility of the animal. The tail suspension test was performed for 6 min as previously described,[32,33] and the duration of immobility was determined for the last 4 min of the test. Immobility was defined as the absence of all except respiratory movement of the mouse. Statistical analysis of the results revealed a significant effect for treatment with tested compound **6**, as shown in Figure 3A. Specifically, ip administration of the antagonist at the dose of 1 mg/kg, but not at 10 mg/kg, induced a decrease in the immobility compared to vehicle.

dx.doi.org/10.1021/jm500880c | J. Med. Chem. 2014, 57, 6879–6884

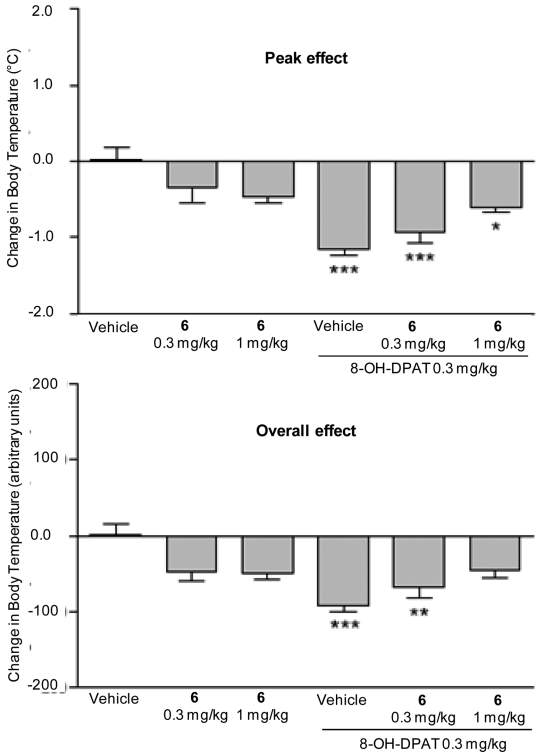

Figure 2. Peak and overall effects of compound **6** in the 8-OH-DPAT-induced hypothermia assay in mice. *P < 0.05, **P < 0.01, ***P < 0.001; one-way analysis of variance followed by Bonferroni's posthoc test. N = 5−7 animals/group.

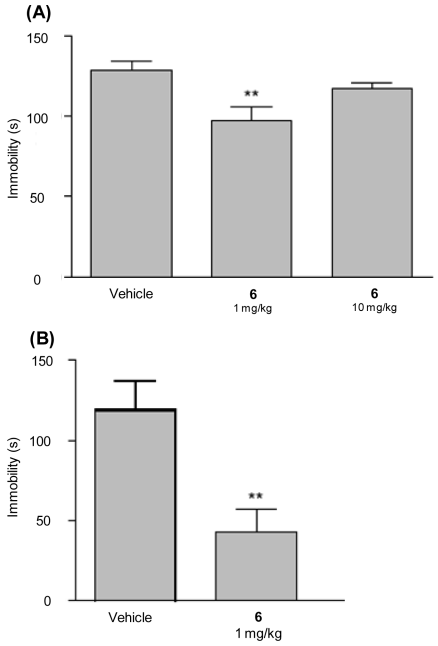

Figure 3. Effects of compound **6** on mouse immobility in the tail suspension test (A) and the forced swim test (B). **P < 0.01; one-way analysis of variance followed by Bonferroni's posthoc test or Student's two-tailed unpaired t test, respectively. N = 7−9 animals/group.

Likewise, the forced swim test was conducted for 6 min as previously described,[19,33] and the duration of immobility was scored for the last 4 min of the test. In this assay, immobility was defined as the absence of all motion except minor movement required for the mouse to keep its head above the water surface. Again, compound **6** significantly reduced immobility at the dose of 1 mg/kg compared to vehicle (Figure 3B).

Therefore, ip administration of compound **6** at the dose of 1 mg/kg induces a decrease in the immobility of mice in the tail suspension and forced swim tests. The observed effects indicate 5-HT_7R antagonist-like properties for ligand **6**, as previous studies have shown that inhibition or inactivation of the 5-HT_7R, using selective antagonists or mice lacking the receptor, leads to reduced immobility in these tests.[12,19,33,34] In addition, it appears that ligand **6** exhibits similar behavior than other 5-HT_7R antagonists in these in vivo models, where an attenuation of the antidepressant activity was observed after administration of a higher dose.[13,19,34] It should also be pointed that **6** displays a high affinity for the 5-HT_7R (K_i = 0.7 nM) and is able to inhibit the in vivo hypothermic effect of 8-OH-DPAT. The specificity of antagonist **6** was further confirmed by the assessment of binding affinity toward other depression-related GPCRs such as the serotonin transporter and 5-HT_{1B}, 5-HT_{2A}, and 5-HT_{2C} receptor subtypes as well as at melatonin MT1 and corticotropin releasing factor CRF1 receptors.[35] Indeed, in all cases, compound **6** (at a concentration of 1 μM) displaced less than the 15% of the corresponding radioligand binding (see data in Table S1 of the Supporting Information), which supports that the observed antidepressant-like effect of compound **6** is mediated by the 5-HT_7R.

In conclusion, the promising in vivo properties exhibited by the new high-affinity and selective 5-HT_7R antagonist described herein reveal its interest as a putative research tool or pharmaceutical in depression disorders.

EXPERIMENTAL SECTION

Computational Model of the Complex between Compound 6 and the 5-HT_7R. MODELER v9.7[36] was used to build a homology model of human 5-HT_7R (Uniprot code P34969) using the crystal structure of human 5-HT_{1B} (PDB code 4IAR)[30] as template. Compound **6** was docked into the receptor model in such a manner that the protonated amine of the ring forms an ionic interaction with D3.32, while the indolone moiety expands toward the extracellular entrance. This structure was placed in a rectangular box containing a lipid bilayer (183 molecules of POPC) with explicit solvent (14334 water molecules) and a 0.15 M concentration of Na^+ and Cl^- ions. This initial complex was energy-minimized and subsequently subjected to a 10 ns MD equilibration, with positional restraints on protein coordinates, to remove possible voids present in protein/lipids or proteins/water interfaces. These restraints were released, and two different replicas of 100 ns MD trajectories were produced at constant pressure and temperature, using the particle mesh Ewald method to evaluate electrostatic interactions. Computer simulations were performed with the GROMACS 4.6.3 simulation package,[37] using the AMBER99SB force field as implemented in GROMACS, Berger parameters for POPC lipids, and the general Amber force field (GAFF) and HF/6-31G*-derived RESP atomic charges for the ligand. This procedure has been previously validated.[38]

General Procedure for the Synthesis of Intermediates 11−15. To a stirred solution of 1,3-dihydro-2*H*-indol-2-one (0.80 g, 6 mmol) and the appropriate dibromide derivative (8 mmol) in anhydrous acetonitrile (90 mL), K_2CO_3 (1.66 g, 12 mmol) was added. The reaction mixture was heated at reflux under an argon atmosphere for 20 h, then cooled to room temperature and filtered. The resulting solution was evaporated under vacuum, and the crude material was resuspended in water and extracted with dichloromethane (3 × 30 mL). The organic layers were dried (Na_2SO_4), filtered, and evaporated under reduced pressure. The obtained residue was purified by column chromatography, using the appropriate eluent, to afford pure **11−15**.

dx.doi.org/10.1021/jm500880c | J. Med. Chem. 2014, 57, 6879−6884

1-[(3*E*)-6-Bromohex-3-en-1-yl]-1,3-dihydro-2*H*-indol-2-one (15). Obtained from 1,3-dihydro-2*H*-indol-2-one and (3*E*)-1,6-dibromohex-3-ene in 60% yield. Chromatography: hexane/EtOAc, from 9:1 to 8.5:1.5. IR (ATR) ν 1711, 1614, 1489, 1466. ^{1}H NMR (300 MHz, $CDCl_3$) δ 2.40 (app q, J = 6.8, 2H, $C\underline{H}_2CH$=), 2.51 (app q, J = 6.8, 2H, $C\underline{H}_2CH$=), 3.29 (t, J = 7.1, 2H, CH_2Br), 3.53 (s, 2H, CH_2CO), 3.75 (t, J = 7.2, 2H, CH_2N), 5.29−5.60 (m, 2H, CH=CH), 6.82 (d, J = 7.7, 1H, CH_{Ar}), 7.02 (t, J = 7.6, 1H, CH_{Ar}), 7.22−7.28 (m, 2H, $2CH_{Ar}$). ^{13}C NMR (50 MHz, $CDCl_3$) δ 29.7, 30.7, 32.4, 35.8, 39.6 ($5CH_2$), 108.7, 122.2, 124.5 (3CH), 124.6 (C), 127.8, 129.3, 129.8 (3CH), 144.5 (C), 175.0 (CO).

General Procedure for the Synthesis of Final Compounds 3−10. To a suspension of the corresponding intermediate **11**−**15** (0.9 mmol) and 1,2,3,4-tetrahydroisoquinoline or (±)-*trans*-decahydroisoquinoline (1.5 mmol) in anhydrous acetonitrile (4 mL), triethylamine was added (0.2 mL, 1.5 mmol). The reaction mixture was heated at 60 °C under an argon atmosphere for 24 h. Upon cooling to room temperature, the solvent was evaporated under reduced pressure and the crude material was resuspended in water and extracted with dichloromethane (3 × 10 mL). The organic layers were dried (Na_2SO_4), filtered, and evaporated, and the resulting oil was purified by column chromatography using the appropriate eluent to provide pure final compounds **3**−**10**.

The free amine was characterized (yield, IR, NMR, MS), dissolved in anhydrous Et_2O (6 mL/mmol), and a commercial 1 M HCl(g)/Et_2O solution (1 mL/mmol) was added. The hydrochloride salt was isolated by filtration or evaporation, washed with anhydrous Et_2O, dried under high vacuum, and characterized (mp, elemental analysis). Satisfactory high pressure liquid chromatography−mass spectrometry (HPLC-MS) analyses confirmed a purity of at least 95% for all final compounds.

1-[(3*E*)-6-(3,4-Dihydroisoquinolin-2(1*H*)-yl)hex-3-en-1-yl]-1,3-dihydro-2*H*-indol-2-one (6). Obtained from **15** and 1,2,3,4-tetrahydroisoquinoline in 80% yield. Chromatography: from EtOAc to EtOAc/EtOH, 9:1; mp 109−111 °C. IR (ATR) ν 1712, 1614, 1489, 1466, 1464. ^{1}H NMR (300 MHz, $CDCl_3$) δ 2.24−2.32 (m, 2H, $C\underline{H}_2CH$=), 2.34−2.42 (m, 2H, $C\underline{H}_2CH$=), 2.50 (t, J = 6.7, 2H, NCH_2), 2.73 (t, J = 5.9, 2H, $CH_{2isoquin}$), 2.90 (t, J = 5.8, 2H, $NCH_{2isoquin}$), 3.51 (s, 2H, CH_2CO), 3.63 (s, 2H, $NCH_{2isoquin}$), 3.75 (t, J = 7.3, 2H, CH_2NCO), 5.50−5.55 (m, 2H, CH=CH), 6.84 (d, J = 7.8, 1H, CH_{ind}), 7.00−7.05 (m, 2H, CH_{ind}, $CH_{isoquin}$), 7.08−7.16 (m, 3H, $3CH_{isoquin}$), 7.23−7.31 (m, 2H, $2CH_{ind}$). ^{13}C NMR (50 MHz, $CDCl_3$) δ 29.0, 30.5, 30.8, 35.8, 39.8, 50.8, 56.0, 58.0 ($8CH_2$), 108.5, 122.1, 124.5 (3CH), 124.6 (C), 125.6, 126.1, 126.6, 127.3, 127.8, 128.7, 131.0 (7CH), 134.3, 135.0, 144.6 (3C), 175.0 (CO). ESI-MS 347.3 $(M + H)^+$. Anal. ($C_{23}H_{26}N_2O\cdot HCl\cdot H_2O$) C, H, N.

In Vivo Evaluation of Compound 6. Male and female 8−12 weeks old C57BL/6J mice obtained from the breeding facilities of The Scripps Research Institute were used in all experiments. The animals were group housed and had free access to standard food pellets and water. The experiments were done in accordance with the Guide for the Care and Use of Laboratory Animals as adopted and promulgated by the U.S. National Institutes of Health and were approved by the Animal Care and Use Committee at TSRI. Every effort was made to reduce the number of animals used and to minimize potential suffering. Compound **6** was dissolved in a small amount of DMSO and then in 0.9% saline. 8-OH-DPAT was dissolved in 0.9% saline. The vehicle 0.9% saline was used as a control. The drugs were administered by single ip injections in the doses indicated. All experiments were started at 9:00 h and are briefly detailed here.

Agonist-Induced Hypothermia Assay. Core body temperature was measured using a rectal probe thermometer (Physitemp BAT-7001H, Physitemp Instruments, Clifton, NJ) as previously described.[32] A basal value was measured immediately before any injection and measurements were then made 15 and 30 min after injection and subsequently every 30 min for a total registration period of 2 h. When the antagonistic properties of **6** were evaluated, it was administered 30 min before the agonist (8-OH-DPAT). Changes in body temperature were determined as peak effect (maximum change during the first 30 min) and overall effect (area under the curve for the entire registration period).

Tail Suspension Test.[19,33] An individual mouse was suspended from the tip of its tail attached with a piece of tape to a metal bar placed horizontally 50 cm above the tabletop. The duration of the test was 6 min, and behavior was scored by a trained investigator. Duration of immobility was determined for the last 4 min of the test. Immobility was defined as the absence of all except respiratory movement. After the test, the animal was returned to its home cage.

Forced Swim Test.[19,33] An individual mouse was placed in a clear plastic cylinder with a diameter of 16 cm. The height of the cylinder was 25 cm, and it was filled with 10 cm of clear water at 25 °C. The duration of the test was 6 min, and behavior was scored by a trained investigator. Duration of immobility was determined for the last 4 min of the test. Immobility was defined as the absence of all movement except minor movement required for the mouse to keep its head above the surface. Afterward, the mouse was towel dried and returned to its home cage. The water was replaced between each animal.

■ ASSOCIATED CONTENT

Ⓢ Supporting Information

Affinity data of **6** toward depression-related GPCRs, chemical general methods, characterization data of compounds **3**−**5**, **7**−**10**, and **14**, elemental and HPLC-MS purity analyses of final compounds **3**−**10**, binding assays at 5-HT_{1A} and 5-HT_7 receptors, and 5-HT_7R AC assay. This material is available free of charge via the Internet at http://pubs.acs.org.

■ AUTHOR INFORMATION

Corresponding Authors

*For M.L.L.-R.: phone, 34-91-3944239; fax, 34-91-3944103; e-mail: mluzlr@quim.ucm.es.

*For L.P.: phone, 34-93-5812797; fax, 34-93-5812344; e-mail: Leonardo.Pardo@uab.es.

Present Address

‖For T.F.: Saint Louis University, Av. del Valle 34, E-28003 Madrid, Spain.

Author Contributions

⊥R.A.M. and H.V.-V. contributed equally.

Notes

The authors declare no competing financial interest.

■ ACKNOWLEDGMENTS

This work was supported by grants from MINECO (SAF2010-22198-C02, SAF2013-48271-C2) and CAM (S2011/BMD2353). R.A.M. and J.C.G.-T. are grateful to MINECO and T.F. to Fundación Ramón Areces for predoctoral fellowships. We thank the NMR Core Facilities from Universidad Complutense de Madrid.

■ ABBREVIATIONS USED

5-HT_7R, 5-HT_7 receptor; AC, adenylate cyclase; ECL, extracellular loop; HPLC-MS, high pressure liquid chromatography−mass spectrometry; MD, molecular dynamics; SSRI, selective serotonin reuptake inhibitor; TM, transmembrane domain

■ REFERENCES

(1) Ruat, M.; Traiffort, E.; Leurs, R.; Tardivel-Lacombe, J.; Diaz, J.; Arrang, J. M.; Schwartz, J. C. Molecular cloning, characterization, and localization of a high-affinity serotonin receptor (5-HT_7) activating cAMP formation. *Proc. Natl. Acad. Sci. U. S. A.* **1993**, *90*, 8547−8551.

(2) Plassat, J. L.; Amlaiky, N.; Hen, R. Molecular cloning of a mammalian serotonin receptor that activates adenylate cyclase. *Mol. Pharmacol.* **1993**, *44*, 229−236.
(3) Hedlund, P. B.; Sutcliffe, J. G. Functional, molecular and pharmacological advances in 5-HT_7 receptor research. *Trends Pharmacol. Sci.* **2004**, *25*, 481−486.
(4) Hedlund, P. B. The 5-HT_7 receptor and disorders of the nervous system: an overview. *Psychopharmacology* **2009**, *206*, 345−354.
(5) Matthys, A.; Haegeman, G.; Van Craenenbroeck, K.; Vanhoenacker, P. Role of the 5-HT_7 receptor in the central nervous system: from current status to future perspectives. *Mol. Neurobiol.* **2011**, *43*, 228−253.
(6) Gellynck, E.; Heyninck, K.; Andressen, K. W.; Haegeman, G.; Levy, F. O.; Vanhoenacker, P.; Van Craenenbroeck, K. The serotonin 5-HT_7 receptors: two decades of research. *Exp. Brain Res.* **2013**, *230*, 555−568.
(7) Brenchat, A.; Ejarque, M.; Zamanillo, D.; Vela, J. M.; Romero, L. Potentiation of morphine analgesia by adjuvant activation of 5-HT_7 receptors. *J. Pharmacol. Sci.* **2011**, *116*, 388−391.
(8) Brenchat, A.; Zamanillo, D.; Hamon, M.; Romero, L.; Vela, J. M. Role of peripheral versus spinal 5-HT_7 receptors in the modulation of pain undersensitizing conditions. *Eur. J. Pain* **2012**, *16*, 72−81.
(9) Cifariello, A.; Pompili, A.; Gasbarri, A. 5-HT_7 receptors in the modulation of cognitive processes. *Behav. Brain Res.* **2008**, *195*, 171−179.
(10) Roberts, A. J.; Hedlund, P. B. The 5-HT_7 receptor in learning and memory. *Hippocampus* **2012**, *22*, 762−771.
(11) Wesolowska, A.; Nikiforuk, A.; Stachowicz, K.; Tatarczynska, E. Effect of the selective 5-HT_7 receptor antagonist SB 269970 in animal models of anxiety and depression. *Neuropharmacology* **2006**, *51*, 578−586.
(12) Guscott, M.; Bristow, L. J.; Hadingham, K.; Rosahl, T. W.; Beer, M. S.; Stanton, J. A.; Bromidge, F.; Owens, A. P.; Huscroft, I.; Myers, J.; Rupniak, N. M.; Patel, S.; Whiting, P. J.; Hutson, P. H.; Fone, K. C.; Biello, S. M.; Kulagowski, J.; McAllister, G. Genetic knockout and pharmacological blockade studies of the 5-HT_7 receptor suggest therapeutic potential in depression. *Neuropharmacology* **2005**, *48*, 492−502.
(13) Abbas, A. I.; Hedlund, P. B.; Huang, X. P.; Tran, T. B.; Meltzer, H. Y.; Roth, B. L. Amisulpride is a potent 5-HT_7 antagonist: relevance for antidepressant actions in vivo. *Psychopharmacology* **2009**, *205*, 119−128.
(14) Cates, L. N.; Roberts, A. J.; Huitron-Resendiz, S.; Hedlund, P. B. Effects of lurasidone in behavioral models of depression. Role of the 5-HT_7 receptor subtype. *Neuropharmacology* **2013**, *70*, 211−217.
(15) Mnie-Filali, O.; Faure, C.; Lambas-Senas, L.; El Mansari, M.; Belblidia, H.; Gondard, E.; Etievant, A.; Scarna, H.; Didier, A.; Berod, A.; Blier, P.; Haddjeri, N. Pharmacological blockade of 5-HT_7 receptors as a putative fast acting antidepressant strategy. *Neuropsychopharmacology* **2011**, *36*, 1275−1288.
(16) Volk, B.; Gacsalyi, I.; Pallagi, K.; Poszavacz, L.; Gyonos, I.; Szabo, E.; Bako, T.; Spedding, M.; Simig, G.; Szenasi, G. Optimization of (arylpiperazinylbutyl)oxindoles exhibiting selective 5-HT_7 receptor antagonist activity. *J. Med. Chem.* **2011**, *54*, 6657−6669.
(17) Berrade, L.; Aisa, B.; Ramirez, M. J.; Galiano, S.; Guccione, S.; Moltzau, L. R.; Levy, F. O.; Nicoletti, F.; Battaglia, G.; Molinaro, G.; Aldana, I.; Monge, A.; Perez-Silanes, S. Novel benzo[*b*]thiophene derivatives as new potential antidepressants with rapid onset of action. *J. Med. Chem.* **2011**, *54*, 3086−3090.
(18) Leopoldo, M.; Lacivita, E.; Berardi, F.; Perrone, R.; Hedlund, P. B. Serotonin 5-HT_7 receptor agents: structure−activity relationships and potential therapeutic applications in central nervous system disorders. *Pharmacol. Ther.* **2011**, *129*, 120−148.
(19) Sarkisyan, G.; Roberts, A. J.; Hedlund, P. B. The 5-HT_7 receptor as a mediator and modulator of antidepressant-like behavior. *Behav. Brain Res.* **2010**, *209*, 99−108.
(20) Wesolowska, A.; Tatarczynska, E.; Nikiforuk, A.; Chojnacka-Wojcik, E. Enhancement of the anti-immobility action of antidepressants by a selective 5-HT_7 receptor antagonist in the forced swimming test in mice. *Eur. J. Pharmacol.* **2007**, *555*, 43−47.
(21) Bonaventure, P.; Dugovic, C.; Kramer, M.; De Boer, P.; Singh, J.; Wilson, S.; Bertelsen, K.; Di, J. N.; Shelton, J.; Aluisio, L.; Dvorak, L.; Fraser, I.; Lord, B.; Nepomuceno, D.; Ahnaou, A.; Drinkenburg, W.; Chai, W. Y.; Dvorak, C.; Sands, S.; Carruthers, N.; Lovenberg, T. W. Translational evaluation of JNJ-18038683, a 5-hydroxytryptamine type 7 receptor antagonist, on rapid eye movement sleep and in major depressive disorder. *J. Pharmacol. Exp. Ther.* **2012**, *342*, 429−440.
(22) López-Rodríguez, M. L.; Porras, E.; Morcillo, M. J.; Benhamú, B.; Soto, L. J.; Lavandera, J. L.; Ramos, J. A.; Olivella, M.; Campillo, M.; Pardo, L. Optimization of the pharmacophore model for 5-HT_7R antagonism. Design and synthesis of new naphtholactam and naphthosultam derivatives. *J. Med. Chem.* **2003**, *46*, 5638−5650.
(23) Medina, R. A.; Sallander, J.; Benhamú, B.; Porras, E.; Campillo, M.; Pardo, L.; López-Rodríguez, M. L. Synthesis of new serotonin 5-HT_7 receptor ligands. Determinants of 5-HT_7/5-HT_{1A} receptor selectivity. *J. Med. Chem.* **2009**, *52*, 2384−2392.
(24) Pittala, V.; Pittala, D. Latest advances towards the discovery of 5-HT_7 receptor ligands. *Mini-Rev. Med. Chem.* **2011**, *11*, 1108−1121.
(25) Pittala, V.; Salerno, L.; Modica, M.; Siracusa, M. A.; Romeo, G. 5-HT_7 receptor ligands: recent developments and potential therapeutic applications. *Mini-Rev. Med. Chem.* **2007**, *7*, 945−960.
(26) López-Rodríguez, M. L.; Benhamú, B.; Morcillo, M. J.; Porras, E.; Lavandera, J. L.; Pardo, L. Serotonin 5-HT_7 receptor antagonists. *Curr. Med. Chem.: Cent. Nerv. Syst. Agents* **2004**, *4*, 203−214.
(27) Venkatakrishnan, A. J.; Deupi, X.; Lebon, G.; Tate, C. G.; Schertler, G. F.; Babu, M. M. Molecular signatures of G-protein-coupled receptors. *Nature* **2013**, *494*, 185−194.
(28) Gonzalez, A.; Cordomi, A.; Caltabiano, G.; Pardo, L. Impact of helix irregularities on sequence alignment and homology modeling of G protein-coupled receptors. *ChemBioChem* **2012**, *13*, 1393−1399.
(29) Wacker, D.; Wang, C.; Katritch, V.; Han, G. W.; Huang, X. P.; Vardy, E.; McCorvy, J. D.; Jiang, Y.; Chu, M.; Siu, F. Y.; Liu, W.; Xu, H. E.; Cherezov, V.; Roth, B. L.; Stevens, R. C. Structural features for functional selectivity at serotonin receptors. *Science* **2013**, *340*, 615−619.
(30) Wang, C.; Jiang, Y.; Ma, J.; Wu, H.; Wacker, D.; Katritch, V.; Han, G. W.; Liu, W.; Huang, X. P.; Vardy, E.; McCorvy, J. D.; Gao, X.; Zhou, E. X.; Melcher, K.; Zhang, C.; Bai, F.; Yang, H.; Yang, L.; Jiang, H.; Roth, B. L.; Cherezov, V.; Stevens, R. C.; Xu, H. E. Structural basis for molecular recognition at serotonin receptors. *Science* **2013**, *340*, 610−614.
(31) Gonzalez, A.; Perez-Acle, T.; Pardo, L.; Deupi, X. Molecular basis of ligand dissociation in β-adrenergic receptors. *PLoS One* **2011**, *6*, e23815.
(32) Hedlund, P. B.; Kelly, L.; Mazur, C.; Lovenberg, T.; Sutcliffe, J. G.; Bonaventure, P. 8-OH-DPAT acts on both 5-HT_{1A} and 5-HT_7 receptors to induce hypothermia in rodents. *Eur. J. Pharmacol.* **2004**, *487*, 125−132.
(33) Hedlund, P. B.; Huitron-Resendiz, S.; Henriksen, S. J.; Sutcliffe, J. G. 5-HT_7 receptor inhibition and inactivation induce antidepressant-like behavior and sleep pattern. *Biol. Psychiatry* **2005**, *58*, 831−837.
(34) Wesolowska, A.; Nikiforuk, A.; Stachowicz, K. Potential anxiolytic and antidepressant effects of the selective 5-HT_7 receptor antagonist SB 269970 after intrahippocampal administration to rats. *Eur. J. Pharmacol.* **2006**, *553*, 185−190.
(35) Catapano, L. A.; Manji, H. K. G protein-coupled receptors in major psychiatric disorders. *Biochim. Biophys. Acta, Biomembr.* **2007**, *1768*, 976−993.
(36) Marti-Renom, M. A.; Stuart, A. C.; Fiser, A.; Sanchez, R.; Melo, F.; Sali, A. Comparative protein structure modeling of genes and genomes. *Annu. Rev. Biophys. Biomol. Struct.* **2000**, *29*, 291−325.
(37) Hess, B.; Kutzner, C.; van der Spoel, D.; Lindahl, E. GROMACS 4: Algorithms for highly efficient, load-balanced, and scalable molecular simulation. *J. Chem. Theory Comput.* **2008**, *4*, 435−447.
(38) Cordomi, A.; Caltabiano, G.; Pardo, L. Membrane protein simulations using AMBER force field and Berger lipid parameters. *J. Chem. Theory Comput.* **2012**, *8*, 948−958.